European Journal of Medicinal Chemistry 224 (2021) 113702

Contents lists available at ScienceDirect

European Journal of Medicinal Chemistry

journal homepage: http://www.elsevier.com/locate/ejmech

# $H_2$dpa derivatives containing pentadentate ligands: An acyclic adjuvant potentiates meropenem activity *in vitro* and *in vivo* against metallo-β-lactamase-producing *Enterobacterales*

Fangfang Chen [a, 1], Mengmeng Bai [a, 1], Wentian Liu [a], Hongtao Kong [a], Tingting Zhang [a], Hong Yao [b], En Zhang [a, *], Juan Du [a, **], Shangshang Qin [a, ***]

[a] School of Pharmaceutical Sciences, Institute of Drug Discovery and Development, Key Laboratory of Advanced Pharmaceutical Technology, Ministry of Education of China, Zhengzhou University, Zhengzhou, 450001, PR China
[b] College of Veterinary Medicine, Henan Agricultural University, Zhengzhou, 450046, PR China

ARTICLE INFO

*Article history:*
Received 31 March 2021
Received in revised form
27 June 2021
Accepted 12 July 2021
Available online 13 July 2021

*Keywords:*
Antibiotic resistance
Metallo-β-lactamase inhibitors
Picolinic acid
*Enterobacterales*

ABSTRACT

The emergence and dissemination of metallo-β-lactamases (MBLs) producing *Enterobacterales* is a great concern for public health due to the limited therapeutic options. No MBL inhibitors are currently available in clinical practice. Herein, we synthesized a series of $H_2$dpa derivatives containing pentadentate-chelating ligands and evaluated their inhibitory activity against MBLs. Related compounds inhibited clinically relevant MBLs (Imipenemase, New Delhi metallo-β-lactamase (NDM) and Verona integron-encoded metallo-β-lactamase) with $IC_{50}$ values of 1–4.9 μM. *In vitro*, the most promising compounds, **5b** and **5c**, which had a chiral methyl at the acid adjacent to **5a**, demonstrated potent synergistic activity against engineered strains, with fractional inhibitory concentration index values as low as 0.07–0.18. The addition of **5b** and **5c** restored meropenem efficacy against 42 MBL-producing *Enterobacterales* and *Pseudomonas aeruginosa* to satisfactory clinical levels. In addition, safety tests revealed that **5b/5c** showed no toxicity in red blood cells, cell lines or mouse model. Further studies demonstrated that compounds **5b** and **5c** were non-competitive MBL inhibitors. *In vivo* compounds **5b** and **5c** potentiated meropenem efficacy and increased the survival rate from 0 to at least 83% in mice with sepsis caused by an NDM-1-positive clinical strain. The activity of the compounds exhibited consistency at the molecular, cellular, and *in vivo* levels. These data indicated that $H_2$dpa derivatives **5b** and **5c** containing pentadentate-chelating ligands may be worthy of further study.



## 1. Introduction

Among β-lactam antibiotics, carbapenems are atypical and have the broadest antibacterial spectrum and strongest antibacterial activity, earning them a vital role in the treatment of multi-drug resistant Gram-negative bacterial infections [1]. However, carbapenems can be hydrolyzed by carbapenemase, a β-lactamase that has a variety of hydrolysis capabilities and the ability to decompose almost all β-lactam antibiotics [2]. Recent nationwide surveillance of carbapenem-resistant *Enterobacterales* (CRE) in China revealed that 85.7% of CRE produce a variety of carbapenemases, indicating that carbapenemase is the most important mechanism conferring carbapenem resistance among clinical *Enterobacterales* isolates [3]. The emergence and spread of carbapenemase-producing *Enterobacterales* (CPE) presents a global threat to public health because of the limited therapeutic options [4].

Two types of carbapenemases, namely class A serine β-lactamases (SBLs) of the KPC type and the zinc-dependent class B metallo-β-lactamases (MBLs), comprising Verona integron-encoded metallo-β-lactamases (VIMs), imipenemases (IMPs) and New Delhi metallo-β-lactamases (NDMs), are regarded as the most important carbapenemases clinically in both *Enterobacterales* and non-fermenting Gram-negative bacilli such as *Acinetobacter* spp. [1]. Since the discovery of the SBL inhibitors sulbactam and tazobactam [5,6], the novel and effective non-β-lactam β-lactamase

* Corresponding author.
** Corresponding author.
*** Corresponding author.
*E-mail addresses:* zhangen@zzu.edu.cn (E. Zhang), dujuan2004@zzu.edu.cn (J. Du), qinshangshang@126.com (S. Qin).
[1] These authors have contributed equally to this work.

https://doi.org/10.1016/j.ejmech.2021.113702
0223-5234/

inhibitors avibactam and vaborbactam [7,8], have recently been introduced into clinical practice. Avibactam and vaborbactam possess broad efficacy against SBLs, particularly KPC, and are as a promising treatment for non-MBL-producing CPE. Unfortunately, no effective inhibitor for MBLs has been approved for clinical use. The development of new antibiotics is progressing at a slower rate than the emergence and spread of CPEs. Therefore, the study of new inhibitors to combat MBL-producing pathogens is vital [9,10]. Unlike SBLs, MBLs use Zn(II) as the active site that catalyzes the hydrolysis of β-lactam antibiotics [11]. Thus, most of the MBL inhibitors interact via coordination to active site zinc ion(s).

To date, multiple structural types of promising MBL inhibitors have been developed, most of which act via active site metal chelation. Examples include the natural product Aspergillomarasmine A (AMA, Fig. 1), an inhibitor of NDM-1 and VIM-2 [12]. Some compounds with inhibitory effects on NDM-1, VIM-2 and IMP-1 that have been investigated include the hypertension drug L-captopril and its isomer D-captopril [13,14]. Others include dipicolinic acid (Fig. 1, **1**) [15] and cyclic boronic acids with similar structures to the β-lactam tetrahedral transition state (Fig. 1, **2**) [16–18], etc [19–22]. Besides, nonmetal binding inhibitors also have been investigated, and these have inhibitory effect on VIM-2 [23]. However, none of these compounds has been approved for clinical use. Most inhibitors currently reported are only evaluated for one type of MBL, with more inhibitors having been evaluated for NDM than for IMP and VIM [24–26]. The existing inhibitors show a high level of enzyme activity but no inhibitory activity at the cellular level; or enzyme activity and inhibitory activity at the cellular level are relatively high but toxicity is also high; or there are no *in vivo* data available [27–29]. Moreover, one of the issues faced in the development of such inhibitors is the biased selectivity toward different MBLs [12,30]. Therefore, safe and effective compounds with good enzyme activity and high cellular and *in vivo* levels against different MBLs are urgently needed.

In recent years, our research group has been committed to discovering new high-efficiency and low-toxicity small molecule antimicrobial peptide mimics [31,32] and inhibitors against NDM-1. In previous studies, we reported some metal chelating agents such as dithiocarbamates that effectively inhibit the enzyme activity of NDM-1 [33,34]. Furthermore, 2-picolinic acid and its derivatives have been evaluated as potential MBL inhibitors. In particular, dipicolinic acid derivatives with different chelating ligands have been reported to exhibit significant inhibitory activity against some MBLs [15,27,35,36]. These include dipicolinic acid with tridentate ligands (DPA, 2,6-pyridine dicarboxylate), which can inhibit MBLs, and $H_2$dedpa (Fig. 2) and its derivatives, which were reported by our research group to exhibit significant inhibitory activity against NDM-1. The next step is to try dipicolinic acid derivatives with other different chelating ligands to discover more potential MBL inhibitors. $H_2$dpa (Fig. 2) derivatives containing pentadentate ligands showed good performance in positron emission tomography imaging [37]. Given this finding, a series of $H_2$dpa derivatives were synthesized and their inhibitory activities against three types of MBLs (including NDM, IMP and VIM) were systematically characterized. Of note, the $H_2$dpa derivatives **5b** and **5c** were demonstrated to be non-competitive MBL inhibitors which were capable of restoring the susceptibility of meropenem (MEM) against clinical isolates producing NDMs and IMP. In addition, the combined use of compounds **5b**/**5c** and MEM improved the survival of septic mice and reduced the bacterial load in mouse organs *in vivo*. Taken together, compounds **5b** and **5c** showed great potential as antibiotic adjuvants and are worthy of further research.

## 2. Results and discussion

### 2.1. Synthesis and characterization

$H_3$dpaa (**5a**) (Fig. 2), with a chiral methyl at the adjacent position of acid analogues **5b** and enantiomer **5c**, and its phosphoric acid analogue **5d** were designed and synthesized. To test the effects of the ethyl acid group of **5a**, the second amine **5e** was used as a control compound. The general synthetic route is shown in Schemes 1 and 2. Compound **2,** which was obtained by selective reduction of a single ester of dimethyl pyridine-2,6-dicarboxylate, reacted with $PBr_3$ to obtain compound **3**. Compounds **4a**-**4e** were then generated from **3** via a double N-alkylation of the primary amine synthon **1a**-**1e** that corresponds to the desired compound (Scheme 1), followed by deprotection in a strong acid to obtain the final products **5a**-**5e** (Scheme 1). The primary amine synthon **1d** required to make **5d** is not commercially available. Accordingly, this compound was synthesized in a single step under mild conditions via an aqueous-mediated catalyst-free aza-Michael addition of diethyl vinyl phosphonate with ammonium hydroxide (see Supporting Information). Of note, the expected compound **5e′** was not obtained, but compound **5e** without the propionic acid structure was achieved (Scheme 2). This may be due to the reverse reaction of Michael addition in the acid reaction system. All final compounds were characterized by $^1$H NMR, $^{13}$C NMR and HRMS. All final compounds possessed a purity of $\geq$ 95% according to HPLC.

### 2.2. Inhibition assays on MBLs

Compounds **5a**,**5b**,**5c**, **5d** and **5e** were assessed to determine their ability to inhibit MBLs (NDM-1, VIM-2 and IMP-1) at the molecular level. Firstly, proteins of NDM-1, VIM-2 and IMP-1 were expressed and purified for detection of the half-maximum inhibitory concentration ($IC_{50}$). The $IC_{50}$ values of compounds (Table 1) revealed that each compound had effective inhibitory activity against all three clinically relevant MBLs (NDM-1, VIM-2 and IMP-1). The functional group on the nitrogen in **5a**-**5e** had little effect on the inhibitory activity against these three enzymes. However, EDTA and AMA had weaker activity against IMP-1, and L-captopril

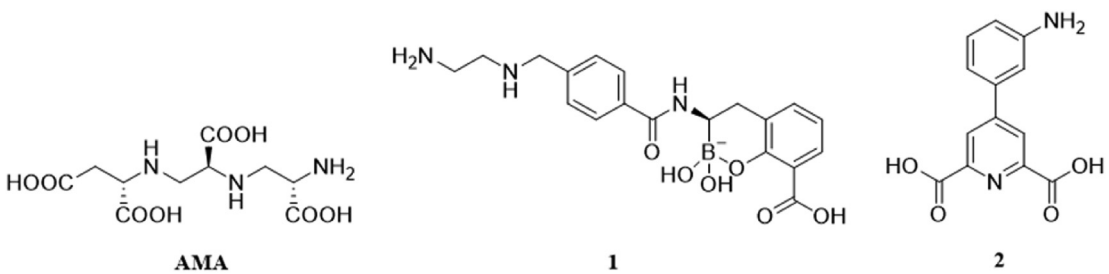


**Fig. 1.** Structures of selected New Delhi metallo-β-lactamase-1 (NDM-1) inhibitors.

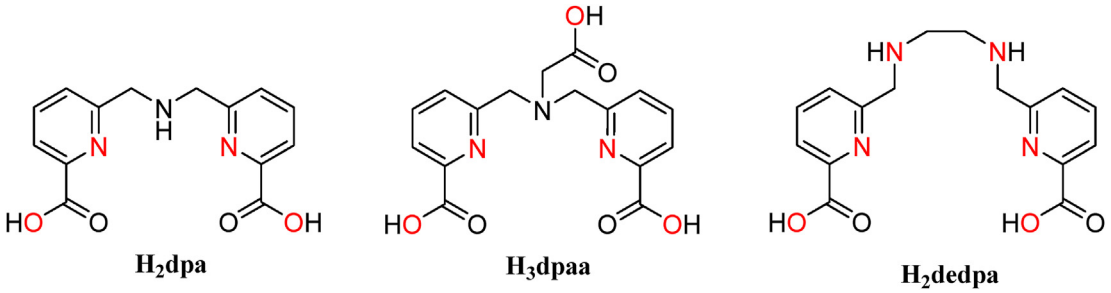


**Fig. 2.** Structure of the selected metal chelator containing different ligands.

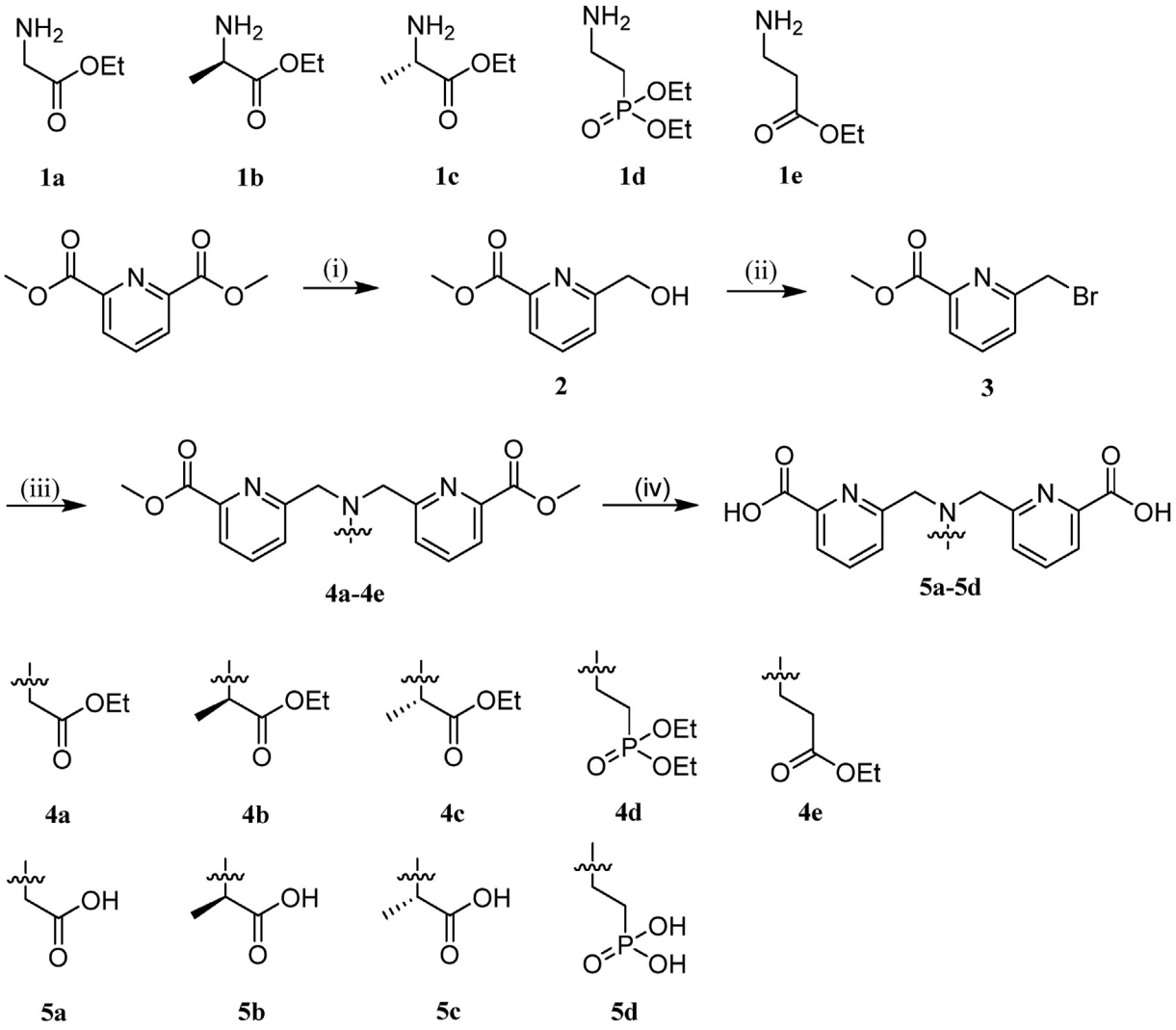


**Scheme 1.** Synthesis of compounds **5a**–**5d**[a]. [a] Reagents and conditions: (i) $NaBH_4$, $CH_3OH$, r.t.; (ii) $PBr_3$, $CHCl_3$, 0°C; (iii) $K_2CO_3$, $CH_3CN$, **1**, 60°C; (iv) 6 M HCl, reflux.

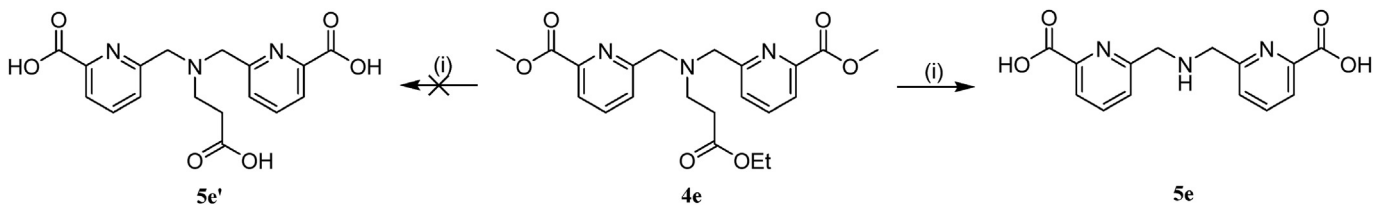


**Scheme 2.** Synthesis of compounds **5e**[a]. [a] Reagents and conditions: (i) 6 M HCl, reflux.

exhibited less effective inhibitory activity against NDM-1. Therefore, the test compounds demonstrated broader enzyme inhibitory activity than the positive control drugs.

### 2.3. Antibacterial activity

#### 2.3.1. Generation of engineered stains (*E. coli*-DH5α/pUC-MBL) for a cell-based screening assay

The recombinant pUC19-based plasmid carrying the $bla_{NDM-1}$/$bla_{IMP-4}$/$bla_{VIM-1}$ gene (Table S1-S2) was introduced into wild-type *Escherichia coli* competent cells DH5α to obtain NDM-1/IMP-4/VIM-1-producing *E. coli* strains that carried no other resistance determinants. Antimicrobial susceptibility testing results showed the minimum inhibitory concentrations (MICs) of MEM against *E. coli*-DH5α/pUC-NDM-1, *E. coli*-DH5α/pUC-IMP-4 and *E. coli*-DH5α/pUC-VIM-1 were 32, 8 and 4 μg/mL, respectively, which were significantly higher than that of *E. coli*-DH5α (0.03125 μg/mL) ($P < 0.05$). This result indicated that the NDM-1/IMP-4/VIM-1-encoding gene had been successfully expressed in the recipient *E. coli*-DH5α cells. These engineered MBL-producing *E. coli* strains were used in a cell-based inhibitor screening assay.

#### 2.3.2. Determination of the FIC values of compounds ***5a*-*5e*** when interacting with *E. coli*-DH5α/pUC-MBL

The synergistic activities of compounds **5a-5e** in combination with MEM against *E. coli*-DH5α-pUC19-MBL strains were initially evaluated by an agar disc diffusion assay. EDTA which can inactivate MBL by chelating out the $Zn^{2+}$ ions, served as a positive control [39]. As shown in Fig. S1 and Fig. S2, all five compounds restored the inhibitory activity of MEM against MBL-producing strains. Next, we performed a standard checkerboard study of the compounds in combination with MEM against *E. coli*-DH5α-pUC19-MBL strains. The MICs of these compounds (**5a-5e**) alone were 128 μg/mL, showing that these inhibitors have no antibacterial activity against the above MBL-producing *E. coli* strains. In addition, the FIC index values, which quantified the degree of interaction between antibiotic and adjuvant, were calculated as described in the experimental methods, with FIC index < 0.5 depicting synergistic interactions. The FIC index values of these compounds on DH5α/pUC-IMP-4 were between 0.14 and 0.38 (Fig. S3B I-VI, reflecting a certain inhibitory effect. These compounds had similar inhibitory effects on *E. coli*-DH5α/pUC-NDM-1 (Fig. S3A I-VI) and *E. coli*-DH5α/pUC-VIM-1 (Fig. S3C I-VI), and the FIC index values of the five compounds were between 0.07 and 0.14. Moreover, the FIC index values of compounds **5b** and **5c** were lower than for other compounds (Fig. S3A II, III, Fig. S3B II, III and Fig. S3C II, III). At low concentrations of **5b** and **5c** (16 μg/mL), the MIC value of MEM for *E. coli*-DH5α/pUC-NDM-1 decreased from 32 to < 0.03125 μg/mL (more than a 1000-fold reduction), showing apparent synergism with FIC index values of 0.07-0.078 (Fig. S3A II, III). Thus, these two compounds (**5b** and **5c**) were selected for further evaluation.

**Table 1**
$IC_{50}$ values of the compounds against NDM-1, VIM-2 and IMP-1.

| Compound | $IC_{50}$ (μM)[a] | | |
|---|---|---|---|
| | NDM-1 | IMP-1 | VIM-2 |
| **5a** | 1.67 ± 0.12 | 1.53 ± 0.11 | 3.88 ± 0.26 |
| **5b** | 1.60 ± 0.02 | 1.56 ± 0.02 | 4.40 ± 0.01 |
| **5c** | 1.69 ± 0.11 | 1.54 ± 0.05 | 4.17 ± 0.12 |
| **5d** | 1.65 ± 0.08 | 2.03 ± 0.04 | 4.84 ± 0.29 |
| **5e** | 1.54 ± 0.09 | 1.05 ± 0.03 | 1.04 ± 0.03 |
| AMA | 4.0 ± 1.0[b] | >200 | 9.6 ± 2.4[b] |
| EDTA | 1.75 ± 0.16 | >200 | 12.5 ± 0.12 |
| L-Captopril | 157.4 ± 0.3[c] | 23.3 ± 1.3[c] | 4.4 ± 0.8[c] |

[a] Values reported as the mean ± SD of at least three independent experiments.
[b] [12].
[c] [38].

#### 2.3.3. Combination studies with MEM against clinical MBL-producing isolates

A total of 50 $bla_{MBL}$ ($bla_{NDM}$, $bla_{IMP}$, $bla_{VIM}$) and $bla_{SBL}$ ($bla_{OXA}$, $bla_{KPC}$) positive Gram-negative clinical bacilli, including 7 *Enterobacter cloacae*, 21 *Escherichia coli*, 17 *Klebsiella pneumoniae*, 2 *Klebsiella oxytoca*, 1 *Citrobacter freundii*, 1 *Enterobacter hormaechei* and 1 *Pseudomonas aeruginosa* strains were selected for evaluation of the antimicrobial activity of **5b/5c** plus MEM (Table S3). The study and consent procedures were approved by the Ethical Committee of Zhengzhou University. The results showed that these compounds did not exert an inhibitory effect on these bacteria even at a dose of 64 μg/mL. The definition of $MIC_{90}$ used in this study was the concentration at which 90% of the bacterial isolates exhibited no growth after 16–20 h of incubated antimicrobial exposure [40]. Significantly, in the presence of **5b**, **5c** or EDTA (16 μg/mL) the $MIC_{90}$ of MEM was 0.25 μg/mL, 0.125 μg/mL and 2 μg/mL, respectively, for clinical strains carrying NDM types NDM-1, NDM-3 or NDM-5 (No. 1–31, No.40-41 in Table S4). In the presence of **5b**, **5c** or EDTA (16 μg/mL) the $MIC_{90}$ of MEM was 1 μg/mL, 0.5 μg/mL and 2 μg/mL, respectively, for clinical strains carrying IMP type IMP-4 (No. 32–41 in Table S4). In the cellular experiments for isolates carrying either NDM or IMP, the inhibitory efficiency of **5b** or **5c** was better than that of EDTA at the same concentration (Table S4). Meanwhile, compound **5b/5c** showed a better inhibitory effect for NDM than IMP producing clinical strains. Such trends were commonly observed regardless of the *Enterobacterales* species, which is consistent with the results of NDM/IMP producing engineered strains (Table S4). For high-level resistant strains carrying NDM-1, the addition of compound **5b/5c** reduced the MIC values of MEM against some strains (No.10 and No.11 in Table S4) by 2048 times or more. However, it was not active against clinical strains that produce SBL (KPC, OXA) (Table S5). These data demonstrated the capability of compounds **5b** and **5c** to effectively potentiate the MEM effect against MBL-harboring Gram-negative bacilli was attributable to their inhibition of MBLs activity.

### 2.4. A potent synergistic effect revealed by time-kill assays

The analysis of bactericidal kinetics clearly reflected the dynamics of MEM combined with inhibitors on the inhibition of bacterial growth in real time. As shown in the time-kill curves in Fig. 3 I-III, the combination of MEM with **5b/5c** dynamically inhibited the growth of bacteria producing MBL. The addition of 16 μg/mL of **5b/5c** to the NDM-1, IMP-4 or VIM-1-producing clinical isolates exposed to an 8 × MIC of MEM for 8 h reduced the population by more than 10,000-fold (Fig. 3 I-II) or to the lowest detection value (Fig. 3 III). After 24 h, the number of bacteria in the clinical isolates producing NDM-1, IMP-4 and VIM-1 was significantly reduced to the lowest detection value or $10^2$ CFU/mL. Accordingly, the broth from the MEM and compound combination group was clear in appearance, compared with a turbid appearance for the control group and the compound and MEM alone groups (Fig.S4 I-III).

### 2.5. Hemolytic activity, toxicity and safety

To determine the toxicity of compounds **5b** and **5c**, their toxicity against red blood cells (RBCs) was initially tested in blood. Lower hemolysis rates of RBCs indicate lower toxicity of the compound. That is, a higher the half value of hemolysis ($HC_{50}$) was taken to indicate lower toxicity of the compound. No hemolysis (0%) and full hemolysis (100%) were observed in the presence of PBS and Triton

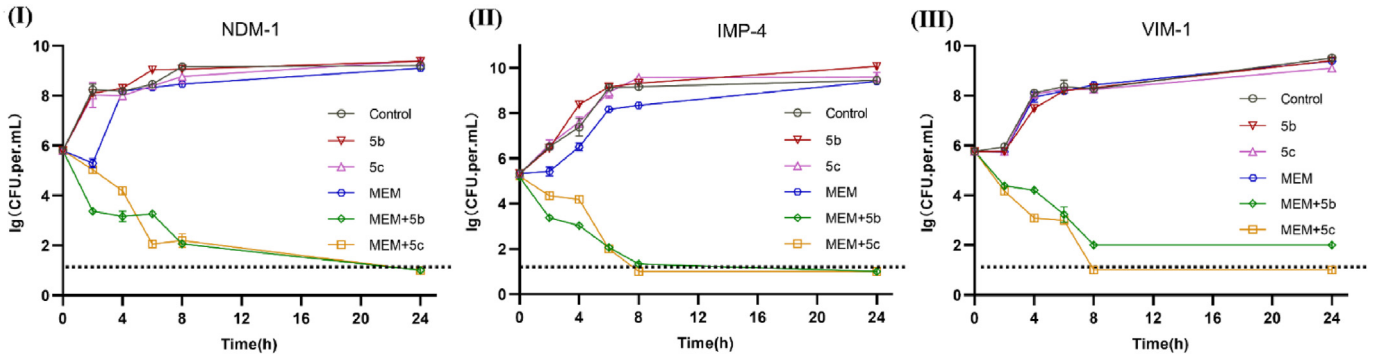


**Fig. 3.** Time-dependent killing of bacterial by MEM combined with compounds **5b** and **5c**. **(I)** No.14 ($bla_{NDM-1}$) strain (Table S4) was challenged with MEM (0.25 μg/mL) or compounds **5b** and **5c** (16 μg/mL) alone or in combination with MEM. **(II)** No.34 ($bla_{IMP-4}$) strain (Table S4) was challenged with MEM (0.25 μg/mL) or compounds **5b** and **5c** (16 μg/mL) alone or in combination with MEM. **(III)** No.42 ($bla_{VIM-1}$) (Table S4) strain was challenged with MEM (1 μg/mL) or compounds **5b** and **5c** (16 μg/mL) alone or in combination with MEM. Microbial concentration: mean ± SD (n = 3). Data represent the mean ± SD from three independent experiments. The symbol "" indicates the detection limit (10 CFU/mL).

X-100, respectively [41,42]. The $HC_{50}$ values of both compounds, **5b** and **5c**, to RBCs compared with Triton X-100 treatment ($HC_{50}$) were greater than 1024 μg/mL, which indicated that compounds **5b** and **5c** were non-hemolytic. Even at a value of 1024 μg/mL, the proportion of hemolysis induced by **5b**/**5c** among RBCs was less than 7% (Fig. 4A).

Subsequently, we evaluated the toxicity of compounds **5b** and **5c** against mammalian cells. A LIVE/DEAD staining method was employed in which green fluorescence represented live cells and red fluorescence represented dead cells. The treated human gastric epithelial (GES) cells exhibited almost exclusively green fluorescence at 32 μg/mL (**5b** and **5c**) (Fig. 4B III-VI), similar to the negative control (Fig. 4B I-II). However, cells treated with the positive control (Triton-X) displayed almost exclusively red fluorescence (Fig. 4B VII-VIII). These results indicated that the MBL inhibitors **5b** and **5c** exhibited low toxicity against GES cells.

The acute toxicity of compounds **5b** and **5c** *in vivo* was determined after intraperitoneal (i.p.) administration of a single dose to BALB/c mice. Different concentrations (50, 30, 20 and 10 mg/kg) of compounds **5b** and **5c** were i.p. injected into the abdominal cavity of BALB/c mice to observe the status and survival rate of the mice as a preliminary examination of the toxicity of the compounds *in vivo*. After injection of compounds **5b** and **5c**, the survival rates of the mice at each concentration remained at 100%, consistent with the normal saline group, within 72 h. This demonstrated that the compounds were less toxic at a concentration of 50 mg/kg.

Next, after i.p. injection of the BALB/c mice with 50 mg/kg of compounds **5b** and **5c**, we obtained blood samples for routine testing and organ (liver, spleen and kidney) tissue sections for hematoxylin and eosin (HE) staining. As shown in Fig. 4C and 24 h after injection, the liver, spleen, and kidneyshowed no obvious pathological changes in the medication group compared with the control group.

Routine blood analysis tested the white blood cell count (WBC), red blood cell count (RBC), hemoglobin (HGB), hematocrit (HCT), mean corpuscular volume (MCV) and platelet count (PLT). The statistical results showed that compared with the normal saline control group, no statistically significant changes in the blood analysis data were detected following the i.p. injection of compounds **5b** and **5c** into BALB/c mice (Fig. 4D). We also collected blood samples for serum biochemical testing and analysis, including albumin (ALB), urea (UREA) and creatinine (CREA). Compared with the normal saline group (Fig. 4D I-IX), when compounds **5b** and **5c** were i.p. injected into BALB/c mice, there was no significant difference in the corresponding indexes of liver and kidney function. These results confirmed that compounds **5b** and **5c** were not toxic and were therefore deemed safe *in vivo*.

### 2.6. Determination of $K_i$ values

To further identify the inhibition model, the inhibition constants $K_i$ of these inhibitors against the NDM-1 enzyme were determined. Next, a steady-state kinetic study was performed on NDM-1, IMP-1 and VIM-2 to explore the inhibition mode of compounds **5b** and **5c** (Table 2). As shown in the Lineweaver-Burk diagram of MBL-catalyzed substrate hydrolysis in Fig. 5, as the concentration of compounds **5b** (Fig. 5A I-III) and **5c** (Fig. 5B I-III) gradually increased, the addition of the compound resulted in a significant decrease in Vmax, indicating that the compound exhibited a non-competitive inhibitory effect. The inference of the $K_i$ value is similar to that of EDTA, AMA and other reported compounds [20].

### 2.7. Testing of zinc homeostasis

To initially explore the mechanism of action of the compound, we performed a zinc ion dependence experiment. When determining the $IC_{50}$ values of compounds **5b** and **5c** on NDM-1, IMP-1 and VIM-2, we noticed that under different concentrations of zinc sulfate (ranging from 0.1 to 100 μM), the $IC_{50}$ values of the compounds also differed (Fig. 6A). This zinc-dependent effect was similar to that of EDTA. By contrast, the inhibitory activity of captopril was not affected by changing the concentration of exogenous zinc added to the assay medium. These findings supported a mechanism of action of compounds **5b** and **5c** based on zinc chelation.

To explore the effects of zinc ions on enzyme activity further, we carried out a zinc inhibition sensitivity experiment using compounds **5b** and **5c** (8 μg/mL) and bacteria containing NDM-1, IMP-4 and VIM-1. Zinc ions were provided by the addition of zinc sulfate. As shown in Fig. 6B I-III, when compounds **5b**, **5c** and MEM were tested alone, the growth rate of bacteria was about 95%, and no antibacterial activity was detected; however, when MEM was used in combination with **5b** or **5c**, the growth of bacteria was reduced to less than 10%. When the amount of zinc ions ranged from 1 μM to 10 μM, the growth of bacteria was inhibited, whereas with a zinc ion concentration of 100 μM, almost 100% bacterial growth was recorded. Furthermore, when the zinc ion concentration was higher than that of compounds **5b** or **5c**, the zinc effect was observed. These data indicated that the activity of compounds **5b** and **5c** was affected by the presence of additional zinc ions.

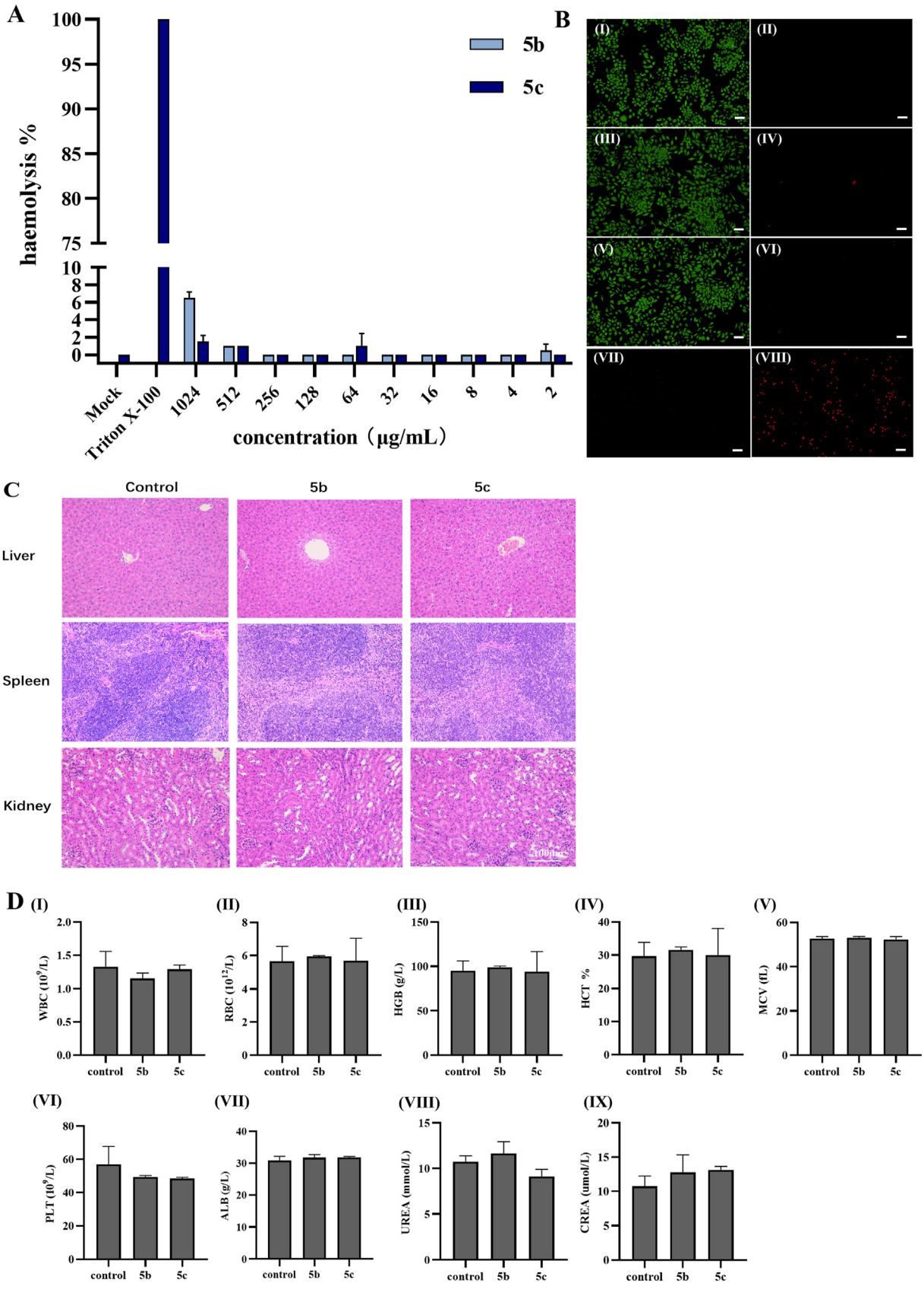


**Fig. 4.** Evaluation of the safety of the compounds *in vivo* and *in vitro*. **(A)** Hemolysis of red blood cells treated with different concentrations of compounds **5b** and **5c**. Mock: treated with phosphate-buffered saline (PBS); Triton X: treated with 0.5% Triton X-100 detergent. Hemolysis rate was the mean ± SD (n = 3). **(B)** Fluorescence microscopy images of GES cells after treatment with compounds **5b** and **5c** for 24 h and staining with calcein AM and propidium iodide. (**I**) Non-treated live cells (negative control); (**II**) non-treated dead cells (negative control); **(III)** live cells treated with compound **5b** (32 μg/mL); **(IV)** dead cells treated with compound **5b** (32 μg/mL); (**V**) live cells treated with compound **5c** (32 μg/mL);

### 2.8. Docking analysis

To verify the possible binding patterns between compounds **5b** and **5c** and NDM-1 enzyme, MOE 2019 software was used to analyze the interface between the inhibitors and the NDM-1 crystal structure (PDB code 4EYL). The virtual docking results are shown in Fig. 7. The dock scores (binding energy) of compounds **5b** and **5c** with NDM-1 were -7.8031 and -7.9433 respectively. In compound **5b**, the carbonyl of one carboxylic acid was bound to two $Zn^{2+}$ ions of NDM-1 via a coordinate bond, and the hydrogen on the other carboxylic acid formed hydrogen bond with Gln123. One of the pyridine groups formed as π-π stacking interaction with His-250 (Fig. 7 I and II). In compound **5c**, the hydroxyl of one of the carboxylic acids bound to the $Zn^{2+}$ ions (ZN302) of NDM-1 via a coordinate bond, and the other carboxylic acid formed two hydrogen bonds with Gln-123 and Glu-152 (Fig. 7 III and IV). These results supported the hypothesis that compounds **5b** and **5c** inhibit NDM-1 by binding to the $Zn^{2+}$ ion. Similar results were obtained in the docking analysis of compounds **5b** and **5c** with IMP-1 (Fig. S5) and VIM-2 (Fig. S6).

### 2.9. In vivo activities of compounds *5b* and *5c*

Compound **5b/5c** enhanced the efficacy of MEM on NDM-1 positive clinical CRE activity, indicating that compound **5b/5c** may restore the clinical efficacy of this antibiotic. To investigate this further, a mouse sepsis model infected with NDM-1-positive extensively drug resistant (XDR) No.12 strain (Table S4) [43] was used to evaluate the potential clinical benefits of compounds **5b** and **5c** combined with MEM against lethal infection *in vivo* (for further data on No.12 strain please see Table S3). As shown in Fig. 8A I-III, BALB/c mice were i.p. infected with a sub-lethal dose of No.12 strain, and combination therapy with compound **5b**/**5c** and MEM showed a significant reduction of the bacterial load detected in the liver, spleen and kidney compared with mice treated with either agent separately. Interestingly, the combined administration group showed improved treatment effects compared with mice treated with either agent or physiological saline separately, demonstrating that a combination of compound **5b**/**5c** and MEM has the therapeutic potential to combat the clinical challenge of NDM-1-producing CRE.

The analysis of HE-stained sections revealed swollen and degenerated liver cells and localized focal necrosis in the control group (Fig. 8B). The central vein was dilated and congested, and inflammatory cell infiltration was occasionally detected, with the red pulp of the spleen mainly being infiltrated with neutrophils. In the MEM (4 mg/kg) and compound **5b/5c** (10 mg/kg) single-use groups, the symptoms were similar to those in control group. In the MEM (4 mg/kg) plus compound **5b/5c** (10 mg/kg) combined treatment group, a complete liver lobule structure was observed, hepatic cords were arranged radially, the central veins were clearly visible, and only a small amount of neutrophil infiltration was seen in the red pulp of the spleen, with the liver and spleen showing significant improvement.

After i.p. injection of the mice with a lethal dose of No.12 strain, MEM and compound **5b**/**5c** monotherapy and combination therapy were initiated. Compound **5b**/**5c** (10 mg/kg) or MEM (4 mg/kg) monotherapy failed to rescue mice within 48 h (Fig. 8C). However, MEM (4 mg/kg) and compound **5b**/**5c** (10 mg/kg) combination therapy rescued at least 83% of mice, who survived to the endpoint of the experiment, 7 days following infection. It is worth mentioning that the MEM plus compound **5b** combination treatment resulted in 100% mouse survival. Effective coadministration of MEM plus compound **5b**/**5c** in mice therefore was translated into *in vivo* efficacy. Furthermore, there are no safety concerns associated with this dual therapy under conditions in which *in vivo* efficacy has been demonstrated.

**Table 2**
$K_i$ determination of the test compounds.

| Compound | $K_i$ (μM)[a] | | |
|---|---|---|---|
| | NDM-1 | VIM-2 | IMP-1 |
| **5b** | 1.59 ± 0.03 | 6.16 ± 0.25 | 1.57 ± 0.01 |
| **5c** | 1.70 ± 0.13 | 5.83 ± 0.52 | 1.54 ± 0.06 |

[a] Values reported as the mean ± SD of at least three independent experiments.

## 3. Experimental

### 3.1. General information

Chemicals were commercially available and were used without further purification unless otherwise stated. All solvents were dried according to standard procedures. The $^1$H NMR and $^{13}$C NMR spectra were recorded at 25°C in $CDCl_3$, $D_2O$, DMSO-$d_6$ or $CD_3OD$ at 600, 400 and 100 MHz, respectively, with TMS as the internal standard. Chemical shifts ($\delta$) are expressed in ppm, and coupling constants J are given in hertz. High-resolution mass spectra (HRMS) data were obtained by ESI on a TOF mass analyzer. Analytical thin layer chromatography (TLC) was performed on glass plates precoated with silica gel to monitor the reactions. Column chromatography was performed on silica gel (300–400 mesh). The purity of each final compound was determined by analytical HPLC on a Water 2695 unit with a C18 column (5 μm, 4.6 × 100 mm).

### 3.2. Synthesis

#### 3.2.1. Methyl 6-(hydroxymethyl)picolinate (*2*) [37]

$NaBH_4$ (7.75 g, 204.95 mmol) was slowly added to the solution of dimethyl pyridine-2,6-dicarboxylate (10.00 g, 51.2 mmol) in MeOH (250 mL) at 0°C in 3 times. The reaction mixture was stirred for 7 h at 0°C. When the reaction was completed, saturated $NaHCO_3$ solution (50 mL) was added and extracted with dichloromethane (200 mL × 3). The organic phase was washed with saturated aqueous NaCl solution (10 mL × 3). The organic phases were dried over anhydrous $MgSO_4$, and evaporated to dryness to give white solid **2** (7.01 g) which was used without purification. Yield: 82%.$^1$H NMR (400 MHz, DMSO-$d_6$) $\delta$ 7.99 (t, $J$ = 7.7 Hz, 1H), 7.96–7.88 (m, 1H), 7.74–7.69 (m, 1H), 5.57 (t, $J$ = 5.9 Hz, 1H), 4.62 (d, $J$ = 5.8 Hz, 2H), 3.87 (s, 3H). $^{13}$C NMR (100 MHz, DMSO-$d_6$) $\delta$ 165.3, 162.5, 146.4, 138.0, 123.8, 123.0, 64.0, 52.3. The spectral data are in accordance with those reported in the literature.

#### 3.2.2. Methyl 6-(bromomethyl)picolinate (*3*) [37]

$PBr_3$ (11.08 g, 40.92 mmol) was added dropwise to the solution of **2** (5.70 g, 34.10 mmol) in chloroform (60 mL) at 0°C. The solution was stirred at room temperature for 4 h. After the reaction was over, saturated sodium bicarbonate was added to adjust pH to 8, extracted with dichloromethane (200 mL × 4). The organic phases

(**VI**) dead cells treated with compound **5c** (32 μg/mL); (**VII**) live cells treated with 0.05% Triton X-100 (positive control); (**VIII**) dead cells treated with 0.05% Triton X-100 (positive control). Scale bar is 200 μm. **(C)** A single dose of compound **5b** (50 mg/kg), compound **5c** (50 mg/kg) or physiological saline was administered to BALB/c mice by intraperitoneal injection. Scale bar is 100 μm. **(D)** Compound blood routine testing and blood biochemical indexes in mice. The data represent the standard errors of three independent experiments (n = 3 for each group).

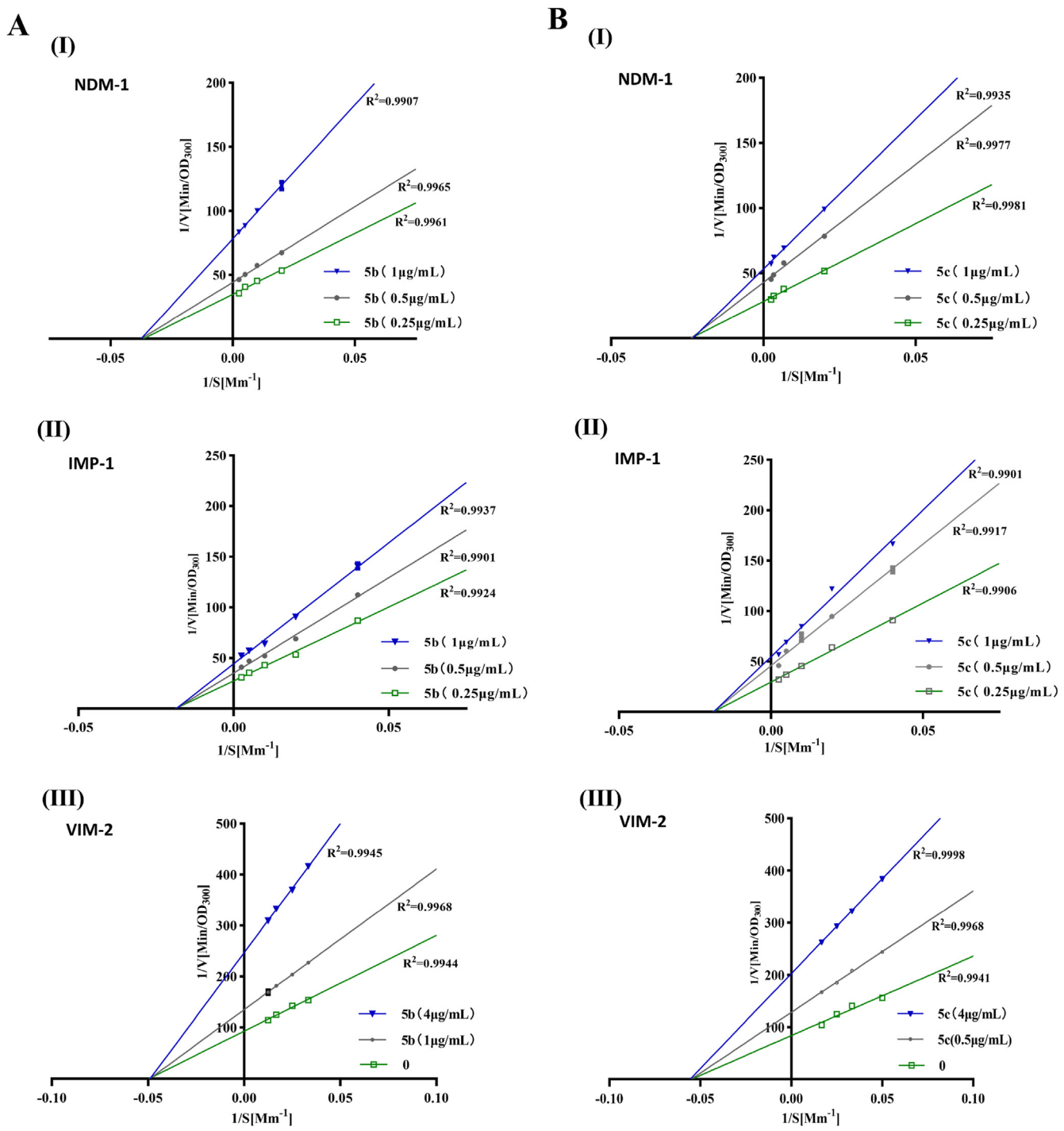


**Fig. 5.** **(A)** Lineweaver–Burk plots of inhibition of MBL hydrolysis activity by compound **5b**. **(B)** Lineweaver–Burk plots of inhibition of MBL hydrolysis activity by compound **5c.**

were washed with brine (20 mL × 3). The organic phases were dried over anhydrous $MgSO_4$, and evaporated to dryness to give light yellow solid **3** (7.61 g). Yield: 97%. $^1$H NMR (400 MHz, DMSO-$d_6$) $\delta$ 8.1–8.0 (m, 2H), 7.8 (dd, $J$ = 7.4, 1.4 Hz, 1H), 4.8 (s, 2H), 3.9 (s, 3H). The spectral data are in accordance with those reported in the literature.

*3.2.3. General procedure for the synthesis compound **4a**-**4e** [44]*

$K_2CO_3$ (0.72 g, 5.21 mmol) and **1** (1.30 mmol) were added to the solution of **3** (0.60 g, 2.60 mmol) in MeCN (6 mL). The reaction mixture was stirred for 12 h at 60°C. After the reaction was over, sodium carbonate was removed by filtration, and the crude reaction mixture was concentrated by rotary evaporation. The crude oil was purified by column chromatography (A: dichloromethane, B: methanol, 100% A to 30% B gradient) to afford compound **4a**-**4e**. Yield: 39%–50%

*3.2.3.1. Dimethyl 6,6'-(((2-ethoxy-2-oxoethyl)azanediyl)bis(-methylene))dipicolinate (**4a**) [37].* **4a**: White solid, $^1$H NMR (400 MHz, $CDCl_3$) $\delta$ 8.0 (dd, $J$ = 7.5, 1.3 Hz, 2H), 7.9–7.8 (m, 4H), 4.2

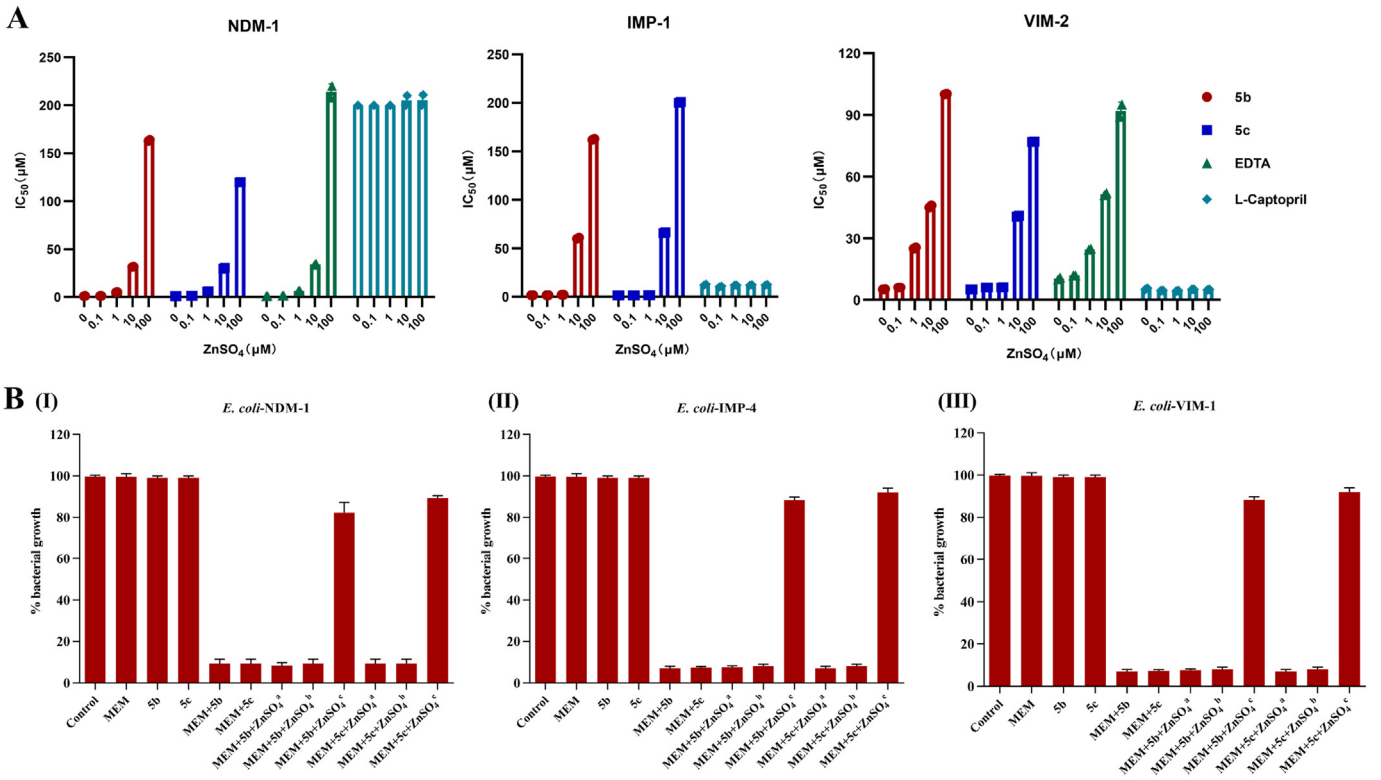


**Fig. 6.** **(A)** The effect of the zinc ion content on the half inhibitory activity of compounds **5b** and **5c** on NDM-1, IMP-1 and VIM-2. **(B)** Metal suppression experiments: control, without drugs; $Zn^{2+}$ was provided by $ZnSO_4$. [a]: compound treated with 1 μM $ZnSO_4$; [b]: compound treated with 10 μM $ZnSO_4$; [c]: compound treated with 100 μM $ZnSO_4$; *E. coli*-MBL refer to *E. coli* DH5α/pUC-NDM-1, *E. coli* DH5α/pUC-IMP-4 and *E. coli* DH5α/pUC-VIM-1 respectively.

(q, $J$ = 7.1 Hz, 2H), 4.1 (s, 4H), 4.0 (s, 6H), 1.3 (t, $J$ = 7.1 Hz, 3H). $^{13}$C NMR (100 MHz, $CDCl_3$) δ 171.1, 165.8, 159.9, 147.4, 137.5, 126.3, 123.8, 60.7, 60.0, 55.3, 52.9, 14.2. Yield: 41%. The spectral data are in accordance with those reported in the literature.

*3.2.3.2. Dimethyl 6,6'-(((1-ethoxy-1-oxopropan-2-yl)azanediyl)bis(methylene)) (R)-dipicolinate (**4b**).* **4b**: White solid, $^1$H NMR (400 MHz, $CDCl_3$) δ 8.0 (d, $J$ = 7.3 Hz, 2H), 7.9 (d, $J$ = 7.3 Hz, 2H), 7.8 (t, $J$ = 7.7 Hz, 2H), 4.2 (q, $J$ = 7.1 Hz, 3H), 4.1 (s, 4H), 4.0 (s, 6H), 3.6 (q, $J$ = 7.1 Hz, 1H), 1.4 (d, $J$ = 7.1 Hz, 3H), 1.3 (t, $J$ = 7.1 Hz, 4H). $^{13}$C NMR (100 MHz, $CDCl_3$) δ 173.5, 165.8, 160.8, 147.3, 137.4, 125.8, 123.6, 60.7, 58.7, 57.1, 52.9, 14.3, 14.0. Yield: 45%. The spectral data are in accordance with those reported in the literature.

*3.2.3.3. Dimethyl 6,6'-(((1-ethoxy-1-oxopropan-2-yl)azanediyl)bis(methylene)) (S)-dipicolinate (**4c**) [45].* **4c**: White solid, $^1$H NMR (400 MHz, $CDCl_3$) δ 8.0 (dd, $J$ = 7.5, 1.3 Hz, 2H), 7.9 (dd, $J$ = 7.9, 1.3 Hz, 2H), 7.8 (t, $J$ = 7.7 Hz, 2H), 4.2 (q, $J$ = 7.1 Hz, 2H), 4.1 (s, 4H), 4.0 (s, 6H), 3.6 (q, $J$ = 7.0 Hz, 1H), 1.4 (d, $J$ = 7.1 Hz, 3H), 1.3 (t, $J$ = 7.1 Hz, 4H). $^{13}$C NMR (100 MHz, $CDCl_3$) δ 173.5, 165.8, 160.8, 147.3, 137.4, 125.8, 123.6, 60.7, 58.7, 57.1, 52.9, 14.3, 14.0. Yield: 50%. The spectral data are in accordance with those reported in the literature.

*3.2.3.4. Dimethyl6,6'-(((2-(diethoxyphosphoryl)ethyl)azanediyl)bis(methylene)) dipicolinate (**4d**) [37].* **4d**: Light gray solid, $^1$H NMR (400 MHz, $CDCl_3$ δ 7.9 (d, $J$ = 8.8 Hz, 2H), 7.8 (d, $J$ = 4.9 Hz, 4H), 4.0–3.9 (m, 4H), 3.9 (s, 6H), 3.9 (s, 4H), 2.9 (q, $J$ = 8.5 Hz, 2H), 2.1–1.9 (m, 2H), 1.2 (t, $J$ = 7.0 Hz, 6H).$^{13}$C NMR (100 MHz, $CDCl_3$) δ 165.7, 159.9, 147.4, 137.5, 126.1, 123.8, 61.6 (d, $J$ = 6.5 Hz), 59.5, 52.9, 47.8, 23.2 (d, $J$ = 137.8 Hz), 16.4 (d, $J$ = 6.1 Hz). Yield: 39%. The spectral data are in accordance with those reported in the literature.

*3.2.3.5. Dimethyl 6,6'-(((3-ethoxy-3-oxopropyl)azanediyl)bis(methylene)) dipicolinate (**4e**) [37].* **4e**: Light yellow oil, $^1$H NMR (400 MHz, $CDCl_3$) δ 8.0 (dd, $J$ = 7.5, 1.3 Hz, 2H), 7.8 (t, $J$ = 7.7 Hz, 2H), 7.8 (dd, $J$ = 7.7, 1.3 Hz, 2H), 4.1 (q, $J$ = 7.1 Hz, 2H), 4.0 (s, 6H), 4.0 (s, 4H), 3.0 (t, $J$ = 7.0 Hz, 2H), 2.6 (t, $J$ = 7.0 Hz, 2H), 1.2 (t, $J$ = 7.1 Hz, 3H). $^{13}$C NMR (100 MHz, $CDCl_3$) δ 172.2, 165.8, 160.1, 147.3, 137.4, 126.0, 123.7, 60.4, 60.0, 52.9, 50.1, 32.8, 14.2. Yield: 47%. The spectral data are in accordance with those reported in the literature.

*3.2.4. General procedure for the synthesis compound **5a**-**5e**. [37]*

Compound **4** (500 μmol) was added 6 M hydrochloric acid (8 mL). The reaction mixture was refluxed for 4 h and evaporate under vacuum to obtain product. The crude product was dissolved in ethanol solvent, acetone was added until no solids precipitate, and a white solid was obtained by filtration. Yield: 53%–73%.

*3.2.4.1. 6,6'-(((carboxymethyl)azanediyl)bis(methylene))dipicolinic acid (**5a**) [44].* **5a**: White solid, mp: 229–230°C. $^1$H NMR (600 MHz, $D_2O$) δ 8.05–7.99 (m, 4H), 7.70 (dd, $J$ = 7.0, 1.8 Hz, 2H), 4.75 (s, 4H), 4.31 (s, 2H). $^{13}$C NMR (100 MHz, $D_2O$) δ 169.6, 166.0, 150.5, 145.8, 141.2, 128.5, 125.4, 58.5, 55.7. HRMS(ESI+): calcd for $C_{16}H_{16}N_3O_6$ $(M + H)^+$ 346.1034, found 346.1040. Yield: 64%. The spectral data are in accordance with those reported in the literature.

*3.2.4.2. (R)-6,6'-(((1-carboxyethyl)azanediyl)bis(methylene))dipicolinic acid (**5b**).* **5b**: White solid, mp: 231–232°C. $^1$H NMR (600 MHz, $D_2O$) δ 7.9–7.8 (m, 4H), 7.6 (d, $J$ = 7.7 Hz, 2H), 4.6 (q, $J$ = 15.0 Hz, 4H), 4.4 (q, $J$ = 7.2 Hz, 1H), 1.7 (d, $J$ = 7.2 Hz, 3H). $^{13}$C NMR (100 MHz, $D_2O$) δ 173.1, 165.9, 151.2, 145.8, 141.2, 128.1, 125.0, 63.2, 56.0, 11.6. HRMS(ESI+): calcd for $C_{17}H_{18}N_3O_6$ $(M + H)^+$ 360.1190, found 360.1198. Yield: 73%.

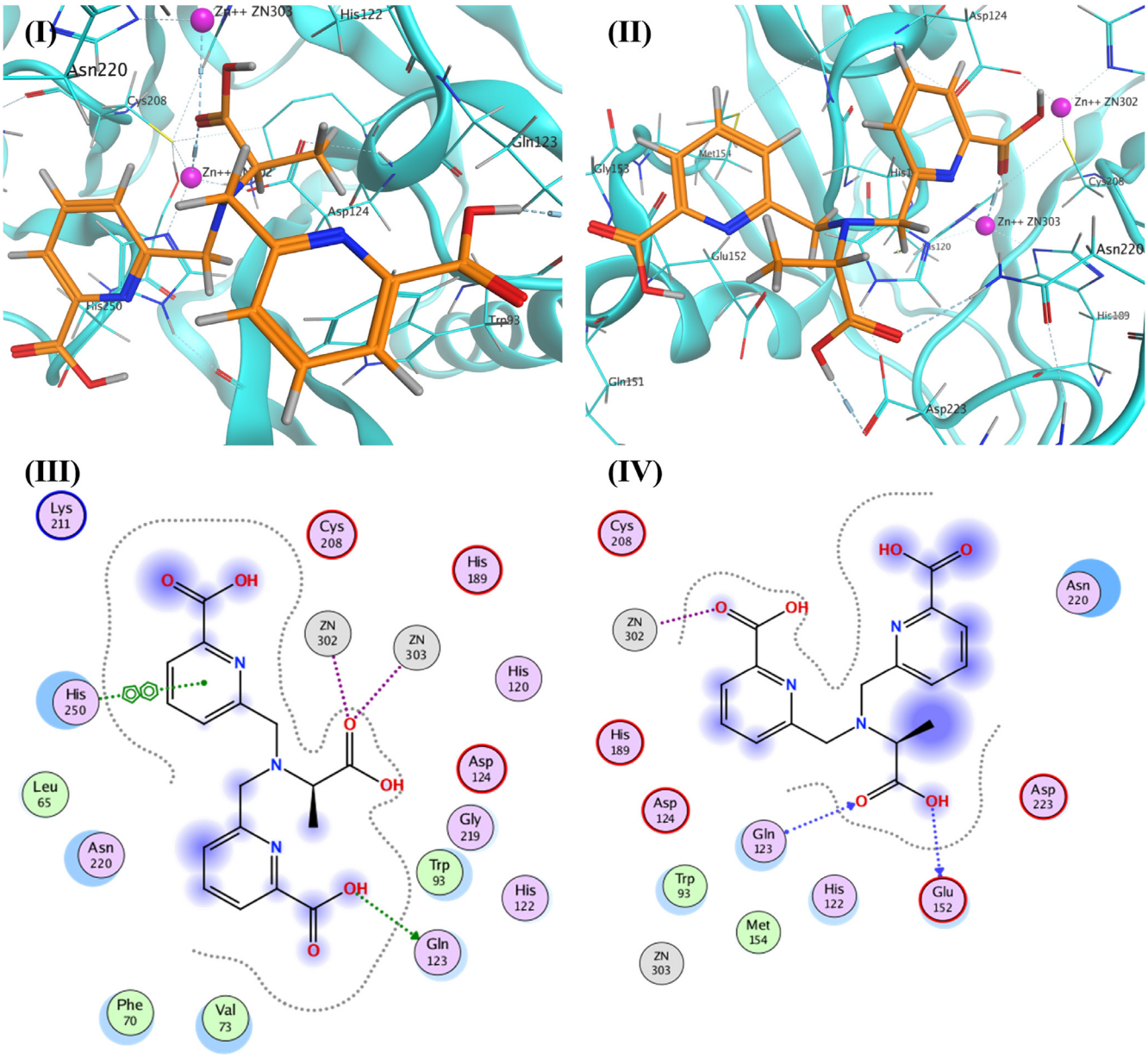


**Fig. 7.** Low energy conformations of compounds **5b** and **5c** docked into NDM-1 (PDB code 4EYL). Locally-enlarged stereoscopic view of compounds **5b** (**I**) and **5c** (**II**) bound to NDM-1. The space represented by the enzyme is colored and the NDM-1 selected residues are displayed by different colored sticks (C, cyan; N, blue; O, red; H, gray). The compounds **5b** and **5c** are shown as sticks colored by atoms (C, orange; N, blue; O, red; H, gray). The enzyme backbone is displayed as a cyan ribbon. Associations with protein residues are indicated by dashed lines. 2D binding models of compounds **5b** (**III**) and **5c** (**IV**) in the active site.

*3.2.4.3. (S)-6,6'-(((1-carboxyethyl)azanediyl)bis(methylene))dipicolinic acid (**5c**) [45].* **5c**: White solid, mp: 233–234°C. $^1$H NMR (600 MHz, $D_2O$) $\delta$ 7.9–7.8 (m, 4H), 7.6 (d, $J$ = 7.7 Hz, 2H), 4.6 (q, $J$ = 15.0 Hz, 4H), 4.4 (q, $J$ = 7.2 Hz, 1H), 1.7 (d, $J$ = 7.2 Hz, 3H). $^{13}$C NMR (100 MHz, $D_2O$) $\delta$ 172.9, 165.9, 151.1, 145.8, 141.1, 128.1, 125.0, 63.2, 56.1, 11.6. HRMS(ESI+): calcd for $C_{17}H_{18}N_3O_6$ $(M + H)^+$ 360.1190, found 360.1199. Yield: 69%. The spectral data are in accordance with those reported in the literature.

*3.2.4.4. 6,6'-(((2-phosphonoethyl)azanediyl)bis(methylene))dipicolinic acid (**5d**) [37].* **5d**: Light yellow, mp: 226–227°C. $^1$H NMR (600 MHz, DMSO-$d_6$) $\delta$ 8.0 (dt, $J$ = 13.6, 7.6 Hz, 4H), 7.8 (d, $J$ = 7.4 Hz, 2H), 4.8 (s, 4H), 3.5 (q, $J$ = 8.9, 8.0 Hz, 2H), 2.3 (dt, $J$ = 18.0, 7.3 Hz, 2H). $^{13}$C NMR (100 MHz, DMSO-$d_6$) $\delta$ 165.7, 151.3, 147.9, 139.4, 128.5, 124.7, 56.9, 50.7, 23.5 (d, $J$ = 132.7 Hz). HRMS(ESI$^+$): calcd for $C_{16}H_{19}N_3O_7P$ $(M + H)^+$ 396.0955, found 396.0963. Yield: 53%. The spectral data are in accordance with those reported in the literature.

*3.2.4.5. 6,6'-(azanediylbis(methylene))dipicolinic acid (**5e**) [37].* **5e**: Light gray solid, mp: 269–270°C. $^1$H NMR (600 MHz, DMSO-$d_6$) $\delta$ 13.1 (s, 2H), 10.1 (s, 2H), 8.2–8.0 (m, 4H), 7.8 (dd, $J$ = 7.5, 1.3 Hz, 2H), 4.6 (s, 4H). $^{13}$C NMR (100 MHz, DMSO-$d_6$) $\delta$ 165.8, 152.4, 147.5, 139.5, 127.4, 124.5, 50.5. HRMS(ESI$^+$): calcd for $C_{14}H_{14}N_3O_4$ $(M + H)^+$ 288.0979, found 288.0984. Yield: 70%. The spectral data are in accordance with those reported in the literature.

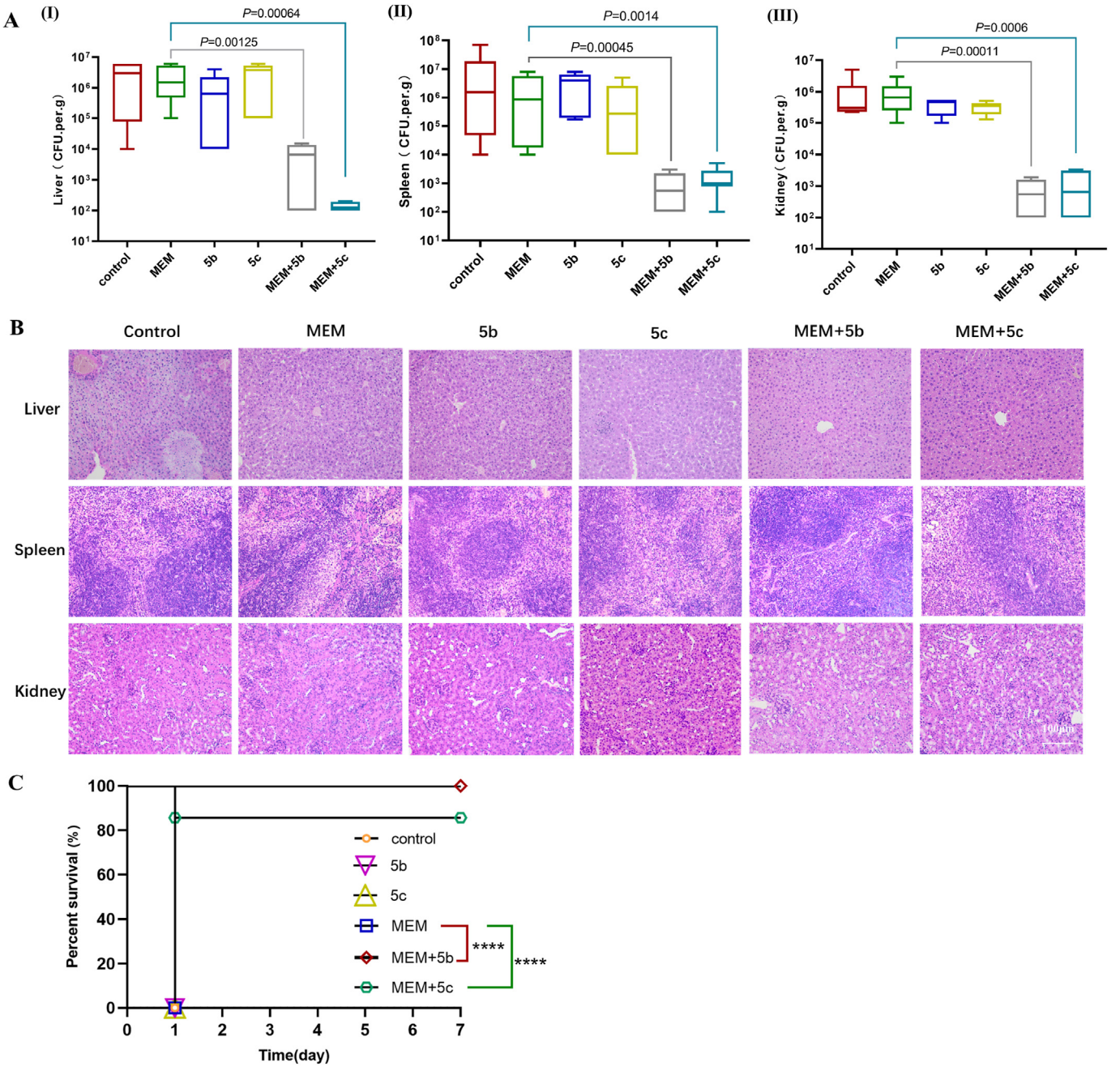


**Fig. 8.** Compounds **5b** and **5c** rescue the activity of MEM *in vivo*. BALB/c mice were administered the NDM-1-positive No.12 strain (MEM MIC 32 μg/mL) by i.p. injection. Each group of mice received a single dose of MEM (4 mg/kg) plus compound **5b** or **5c** (10 mg/kg) or saline. **(A)** For BALB/c mice injected with a sub-lethal dose ($1 \times 10^7$ CFU) of No.12 strain, the bacterial loads in the liver **(I)**, spleen **(II)** and kidney **(III)** were detected. A single dose of MEM, compound **5b**, compound **5c** or MEM plus compound **5b** and compound **5c**, was injected into the abdominal cavity for treatment. Data represent the mean and standard error from two separate experiments (n = 6 per group). **(B)** HE staining results from BALB/c mice injected with a sub-lethal dose ($1 \times 10^7$ CFU) of No.12 strain. A single dose of MEM, compound **5b**, compound **5c**, or MEM plus compound **5b** and compound **5c**, was injected into the abdominal cavity for treatment. **(C)** In the survival experiment, BALB/c mice were injected with a lethal dose ($5 \times 10^7$ CFU) of No.12 strain. A single dose of MEM, MEM plus compound **5b** and compound **5c** alone, or saline was injected for treatment. (n = 6 per group) ****$P < 0.0001$. $P$ values < 0.05 were considered statistically significant.

### 3.3. Biological activity

#### 3.3.1. $IC_{50}$ enzyme inhibition assays

Enzyme (NDM-1, 50 nM; VIM-2, 500 pM; IMP-1, 50 nM) was mixed with substrate (120 μM MEM for NDM-1; 20 μM Nitrocefin (NIT) for VIM-2; 120 μM Imipenem (IPM) for IMP-1) after a 5–10 min preincubation with compounds and linear portions of curves were used to analyze data. Assays were read in 96-well microplate format at 300 nm (486 nm for NIT) using a Spectramax reader (Molecular Devices) at 30°C. The assay was performed in 10 mM HEPES pH 7.5, 200 mL final volume.

#### 3.3.2. Expression and purification of MBLs enzyme

The pET-28a-NDM-1, VIM-2, IMP-1 plasmids were introduced into the expression strains *E. coli* BL21(DE3), inoculated in 15 mL of LB liquid medium containing 35 μg/mL kanamycin, and cultured at 37°C with shaking for 12 h. Expand culture in 800 mL of LB containing 35 mg/mL kanamycin at 37°C. When $OD_{600}$ reached 1.0, add

0.5 mM per 100 mL transfer cultures of IPTG, 20°C to cultivate the 16 h. After induction, centrifuged at 4600 g at 16°C for 8 min, lysate buffer (20 mM Tris pH = 7.5, 300 mM NaCl) washing twice. Added about 100 mL of lysate buffer to the bacterial pellet and blow evenly to a sterile mass. At the same time, 1/1000 of β-ME (protected disulfide bond) and PMSF (inhibited protease) were added. Crushed the cells and centrifuge for 50–60 min at 13500 g at 4°C. Divided the filtered liquid and grate into centrifuge tubes containing HisPur Ni-NTA resin, and shook for 1 h at the lowest speed at 4°C. The mixture was allowed to stand for 30 min at 4°C. Rinse the grate with lysis solution (pH = 7.5). Washed the contaminated protein with washing buffer (lysate containing 10 mM imidazole), and then purified the protein with elution buffer (containing 250 mM imidazole). Run SDS-PAGE to detect the concentration and content of protein. Then used desalting column for replacing MBLs, measured the protein content, and store the enzyme at -80°C.

### 3.3.3. Standard agar disc diffusion assay

The MIC was determined by the microdilution method according to the Clinical and Laboratory Standards Institute (CLSI) guidelines [46]. In short, spread $1 \times 10^5$ CFU of bacteria on the MH plate, waited for the semi-dry sticker, and then dropped the meropenem (10 μg) and tested the compound (0.1 mM, 10 μL) on the respective paper. The test plate was incubated at 37°C for 16–20 h. According to CLSI standards, when MEM was used as an antimicrobial compound, a single inhibition zone < 14 mm was resistant and > 18 mm was sensitive.

### 3.3.4. Susceptibility testing

MICs were determined by the microdilution method according to the CLSI guidelines [46]. In short, $1 \times 10^5$ CFU bacterial cells were inoculated in 100 μL of cation-adjusted Mueller Hinton broth containing β-lactam and appropriately diluted inhibitor. The final concentration of DMSO was kept below 1% in the measurement. The tested plates were then incubated at 37°C for 16–20 h. The MIC value was determined as the lowest concentration of lactam tested in the absence of visible bacterial growth. Use a microplate reader to read the optical density at 600 nm to draw the heat maps. The FIC index value was calculated using the following formula:

$$FIC\ index = \frac{\text{MIC of β"TT5843c571""ADlactam with inhibitor}}{\text{MIC of β"TT5843c571""ADlactam alone}} + \frac{\text{MIC of inhibitor with β"TT5843c571""ADlactam}}{\text{MIC of inhibitor alone}}$$

If the MIC of the individual inhibitor was > 128 μg/mL, the concentration of "MIC of the individual inhibitor" was set to 128 μg/mL to determine the FIC index value. Unless otherwise stated, the FIC index was defined as the lowest value among all obtained values. Synergy was defined as the effect observed when the FIC index value was ≤ 0.5.

### 3.3.5. Time-dependent killing

A time-kill assay was performed to further determine the synergistic effect of compounds **5b** and **5c** with β-lactam antibiotics according to the method as previously described [34]. Either MEM (4 MIC) alone or **5b** and **5c** (16 μg/mL) alone or a combination of the two was added to the bacterial solution, and then incubation was performed at 37°C. At 0, 2, 4, 6, 8, and 24 h after adding the agents, an aliquot of bacterial culture was removed, diluted, and spotted on MH agar plates to count the viable bacterial cells.

### 3.3.6. Hemolytic activity

According to the method as previously described [34], fresh sterile sheep blood (provided by the China Nanjing Bian Zhen biology Technology Co., Ltd, excellent grade GR), was suspended with 1 × PBS and centrifuged (220 g, 10 min) to remove excess impurities. The treated red blood cells were diluted and tested with the resulting 5% erythrocyte suspension. DMSO or water as the solvent (final concentration of no more than 0.5%) in each experiment were hemolytic determination to prevent appearance of false positive results. The Triton-X detergent at 0.5% was used as the positive control. The 5% erythrocyte suspension was placed in a 96-well plate of 150 μL/well. The drug was diluted in a sterile EP tube using 1 × PBS, 50 μL/well was added and each sample was tested in parallel using three duplicate wells under the same concentration. After incubation at 37°C for 1 h, the plates were placed in a 4°C centrifuge (1150 g, 5 min).100 μL of the supernatant in each hole was transferred to a new 96-well plate. Eventually, the results were measured at 540 nm on the microplate reader. Percentage of hemolytic was determined as $(A - A_0)/(A_{total} - A_0) \times 100$, and A was the test well, $A_0$ was the negative control, and $A_{total}$ was the positive.

### 3.3.7. Fluorescence microscopy

GES cells with good growth were tested. The cells were homogeneously cultured in 24-well plates, and the cells were incubated for 24 h and then the test compound was added at the different concentration. According to the mild destruction of the cell membrane by 0.05% Triton-X, use the PI to detection the dead cells. The reason is when the cells treated with the 0.05% Triton-X, PI can be easily combined with the DNA in the nucleus. The PI-DNA complex will release red fluorescence when the excitation and emission wavelengths are 535 nm and 615 nm respectively. However, in the living cells, the non-fluorescence of Calcium-AM is converted to green fluorescence of calcium after the esterase of the cells is hydrolyzed by hydroxymethyl ester. There is no such process for dead cells. Cells treated with 0.1% Triton-X was the positive control. After 24 h, the solution with 1 × PBS and stained with 2 μM Calcein-AM (Sigma-Aldrich) or 4.5 μM propidium iodide (PI, Aladdin) was added and incubated for 15 min in a sterile environment. In the end, the solution contains Calcein-AM: PI = 1: 1. At last, 1 × PBS was used to wash the plate with the dead cells in the collection and were added to the corresponding wells. Images were captured with 20 × objective in Nikon 901 fluorescence microscope.

### 3.3.8. Zinc Dependency assay

We added MBL enzyme (NDM-1, 50 nM; VIM-2, 500 pM; IMP-1, 50 nM) together with the dissolved compound to a 96-well plate and incubated for 5 min according to the method as previously described [27]. After that, substrates (120 μM MEM for NDM-1; 20 μM NIT for VIM-2; 120 μM IPM for IMP-1) containing different final concentrations of zinc sulfate (0.1, 1, 10, and 100 μM) were added to the wells, and the $IC_{50}$ of compounds **5b** and **5c** were evaluated.

The test of zinc homeostasis experiments were had done according to the experiment of the influence of zinc ion content on enzyme activity [47]. We carried out the zinc inhibition sensitivity experiment of compounds **5b** and **5c** to bacteria containing NDM-1, IMP-4 and VIM-1. Similarly, zinc ions were provided by adding zinc sulfate. The experimental operation was the same except that different amounts of $ZnSO_4$ was added respectively. Eventually, the results were measured at the $OD_{600}$ nm of the microplate reader. The test results were plotted as the mean ± SD of the three samples.

### 3.3.9. $K_i$ value determination

Compounds **5b** and **5c** were used for *in vitro* inhibition determination of MBL. Mix MBL enzyme (NDM-1, 50 nM; VIM-2, 500 pM; IMP-1, 50 nM) with different concentrations of inhibitors **5b** and **5c**, and incubate at 30°C for 5 min. Add the corresponding substrate (MEM corresponds to NDM-1 to make the concentration

reach 120 μM, IPM corresponds to IMP-1 to make the concentration reach 120 μM, and NIT corresponds to VIM-2 to make the concentration reach 20 μM) and monitor at 300 nm The hydrolysis rate of each substrate (NIT was 486 nm). All reactions were performed in 10 mM HEPES (pH 7.5) buffer.

*3.3.10. Molecular docking studies*

The protein complexes used for this study were obtained from protein data bank (PDB code: 4EYL), and all water molecules were eliminated. Hydrogen and partial charges were added by the protonate 3D program of MOE 2019; Energy minimization of the ligand was carried out using energy minimize program of MOE. Default parameter settings generated by the program of MOE were used for docking.

*3.3.11. In vivo safety animal experiment*

Female BALB/c mice weighing 15–17 g, age 7–9 weeks, purchased from Beijing Weitong Lihua Laboratory. Material Technology Co., Ltd. (SCXK (Beijing) 2016-0006, Beijing, China).

The drug safety evaluation experiment was to determine the acute toxicity of compound **5b** and **5c** *in vivo* by single-dose intraperitoneal injection of mice, and tissue staining to check the safety of the compounds [20]. In the acute toxicity experiment, mice were divided into 9 groups, each with 6 mice, and different concentrations of compounds were injected intraperitoneally to observe the 72-h survival rate and survival status of the mice.

The tissue staining experiment was to divide the mice into 3 groups, 3 in each group, control (normal saline, intraperitoneal injection), **5b** (50 mg/kg, intraperitoneal injection) and compound **5c** (50 mg/kg, intraperitoneal injection). 24 h after injection, these mice were euthanized and dissected. The organs (liver, spleen and kidney) of the mice were sectioned and stained with HE.

The blood routine experiment is to divide the mice into 3 groups, 3 in each group, control (normal saline, intraperitoneal injection), **5b** (50 mg/kg, intraperitoneal injection) and compound **5c** (50 mg/kg, intraperitoneal injection). 24 h after the injection, blood was taken for routine testing in each group.

*3.3.12. In vivo sepsis animal experiment*

Female BALB/c mice weighing 15–17 g, age 7–9 weeks, purchased from Beijing Weitong Lihua Laboratory. Material Technology Co., Ltd. (SCXK (Beijing) 2016-0006, Beijing, China).

We established a mouse sepsis model to evaluate the therapeutic effects of compounds **5b** and **5c** [12]. For this organ loading experiment, the mice were randomly divided into 9 mice in each group. A sublethal dose of *K. pneumoniae* ($1 \times 10^7$ CFU) was given to BALB/c mice by intraperitoneal injection. Thirty minutes after the injection, a single dose of MEM (4 mg/kg), a single dose of compound (10 mg/kg) and a combination of MEM (4 mg/kg) plus compound (10 mg/kg) were treated, and the state of the mice was observed for 2 days, And dissected the mice to take out the liver, spleen and kidney, and counted the homogenized organs of 6 mice. The other 3 mice were sent tissue sections for HE staining.

For this survival rate experiment, we randomly divided the mice into 6 cages per group. The lethal dose of *K. pneumoniae* ($5 \times 10^7$ CFU) was given to BALB/c mice by intraperitoneal injection. After 30 min of injection, a single dose of MEM (4 mg/kg), a single dose of compound (10 mg/kg), and a combination of MEM (4 mg/kg) plus compound (10 mg/kg) were treated, and the survival of mice was observed for 7 days state and calculate the survival rate to draw a survival curve.

## 4. Conclusions

A series of $H_2$dpa derivatives containing pentadentate chelating ligands were prepared and found to have inhibitory activity against MBLs (NDM, VIM and IMP) at the molecular, cellular and *in vivo* level. *In vitro*, compounds **5b** and **5c** had low FIC values against engineered strains (*E. coli*-DH5α/pUC-NDM-1, *E. coli*-DH5α/pUC-IMP-4 and *E. coli*-DH5α/pUC-VIM-1), and restored the activity of MEM against clinical strains containing MBLs. In addition, compounds **5b** and its enantiomer **5c** exhibited a low level of RBC hemolysis and cytotoxicity, and were considered safe in mice. It was speculated that the compound exerted its activity in a non-competitive manner by chelating zinc ions. Compared with the MEM group in the sepsis model, combination therapy with MEM and **5b**/**5c** was successful in reducing bacterial loads in the organs and improving the survival rate in mice infected with NDM-1-producing *K. pneumoniae* clinical isolates. Compound **5b** combined with MEM was particularly successful, resulting in a survival rate of 100%. The results herein suggest that compounds **5b** and **5c** warrant further investigation as a novel combination treatment.

## Statement

The studies involving human participants were reviewed and approved by the Ethical Committee of Zhengzhou University. Written informed consent to participate in this study was provided by the participants' legal guardian/next of kin. All animal studies were approved by the Life Science Ethics Review Committee of Zhengzhou University, and were conducted in compliance with European guidelines for the care and use of laboratory animals, all experiments were performed in a manner that minimized animal suffering.

## Declaration of competing interest

The authors declare that they have no known competing financial interests or personal relationships that could have appeared to influence the work reported in this paper.

## Acknowledgments

This research was financially supported by the National Natural Science Foundation of China (Nos. 21702190).

## Appendix A. Supplementary data

Supplementary data related to this article can be found at https://doi.org/10.1016/j.ejmech.2021.113702.

## References

[1] D. Hammoudi Halat, C. Ayoub Moubareck, The current burden of carbapenemases: Review of significant properties and dissemination among gram-negative bacteria, Antibiotics 9 (2020) 186, 186.
[2] L.Y. Hsu, A. Apisarnthanarak, E. Khan, N. Suwantarat, A. Ghafur, P. Tambyah, Carbapenem-resistant *Acinetobacter baumannii* and *enterobacteriaceae* in south and southeast asia, Clin. Microbiol. Rev. 30 (2017) 1–22.
[3] Q. Wang, X. Wang, J. Wang, P. Ouyang, C. Jin, R. Wang, Y. Zhang, L. Jin, H. Chen, Z. Wang, F. Zhang, B. Cao, L. Xie, K. Liao, B. Gu, C. Yang, Z. Liu, X. Ma, L. Jin, X. Zhang, S. Man, W. Li, F. Pei, X. Xu, Y. Jin, P. Ji, H. Wang, Phenotypic and genotypic characterization of carbapenem-resistant *enterobacteriaceae*: data from a longitudinal large-scale CRE study in China (2012-2016), Clin. Infect. Dis. 67 (2018) S196–s205.
[4] R. Han, Q. Shi, S. Wu, D. Yin, M. Peng, D. Dong, Y. Zheng, Y. Guo, R. Zhang, F. Hu, Dissemination of carbapenemases (KPC, NDM, OXA-48, IMP, and VIM) among carbapenem-resistant *enterobacteriaceae* isolated from adult and children patients in China, Front. Cell. Infect. Microbiol. 10 (2020) 314.
[5] M. Akova, Sulbactam-containing beta-lactamase inhibitor combinations, Clin. Microbiol. Infect. 14 (2008) 185–188.
[6] R.C. Xamplas, G.S. Itokazu, R.C. Glowacki, A.E. Grasso, C. Caquelin, D.N. Schwartz, Implementation of an extended-infusion piperacillin-tazobactam program at an urban teaching hospital, Am. J. Health Syst. Pharm. 67 (2010) 622–628.

[7] D. van Duin, R.A. Bonomo, Ceftazidime/avibactam and ceftolozane/tazobactam: second-generation β-Lactam/β-Lactamase inhibitor combinations, Clin. Infect. Dis. 63 (2016) 234–241.

[8] G.G. Zhanel, C.K. Lawrence, H. Adam, F. Schweizer, S. Zelenitsky, M. Zhanel, P.R.S. Lagacé-Wiens, A. Walkty, A. Denisuik, A. Golden, A.S. Gin, D.J. Hoban, J.P. Lynch 3rd, J.A. Karlowsky, Imipenem-Relebactam and meropenem-vaborbactam: two novel carbapenem-β-lactamase inhibitor combinations, Drugs 78 (2018) 65–98.

[9] K. Bush, P.A. Bradford, Interplay between β-lactamases and new β-lactamase inhibitors, Nat. Rev. Microbiol. 17 (2019) 295–306.

[10] Y.H. Yan, G. Li, G.B. Li, Principles and current strategies targeting metallo-β-lactamase mediated antibacterial resistance, Med. Res. Rev. 40 (2020) 1558–1592.

[11] S.E. Boyd, D.M. Livermore, D.C. Hooper, W.W. Hope, Metallo-β-Lactamases: structure, function, epidemiology, treatment options, and the development pipeline, Antimicrob. Agents Chemother. 64 (2020) e00397-00320.

[12] A.M. King, S.A. Reid-Yu, W. Wang, D.T. King, G. De Pascale, N.C. Strynadka, T.R. Walsh, B.K. Coombes, G.D. Wright, Aspergillomarasmine A overcomes metallo-beta-lactamase antibiotic resistance, Nature 510 (2014) 503–506.

[13] F.-M. Klingler, T.A. Wichelhaus, D. Frank, J. Cuesta-Bernal, J. El-Delik, H.F. Müller, H. Sjuts, S. Göttig, A. Koenigs, K.M. Pos, D. Pogoryelov, E. Proschak, Approved drugs containing thiols as inhibitors of metallo-β-lactamases: strategy to combat multidrug-resistant bacteria, J. Med. Chem. 58 (2015) 3626–3630.

[14] Y. Yusof, D.T.C. Tan, O.K. Arjomandi, G. Schenk, R.P. McGeary, Captopril analogues as metallo-β-lactamase inhibitors, Bioorg. Med. Chem. Lett 26 (2016) 1589–1593.

[15] A.Y. Chen, P.W. Thomas, A.C. Stewart, A. Bergstrom, Z. Cheng, C. Miller, C.R. Bethel, S.H. Marshall, C.V. Credille, C.L. Riley, R.C. Page, R.A. Bonomo, M.W. Crowder, D.L. Tierney, W. Fast, S.M. Cohen, Dipicolinic acid derivatives as inhibitors of New Delhi metallo-β-lactamase-1, J. Med. Chem. 60 (2017) 7267–7283.

[16] J. Brem, R. Cain, S. Cahill, M.A. McDonough, I.J. Clifton, J.-C. Jiménez-Castellanos, M.B. Avison, J. Spencer, C.W.G. Fishwick, C.J. Schofield, Structural basis of metallo-β-lactamase, serine-β-lactamase and penicillin-binding protein inhibition by cyclic boronates, Nat. Commun. 7 (2016) 12406.

[17] A. Krajnc, J. Brem, P. Hinchliffe, K. Calvopiña, T.D. Panduwawala, P.A. Lang, J.J.A.G. Kamps, J.M. Tyrrell, E. Widlake, B.G. Saward, T.R. Walsh, J. Spencer, C.J. Schofield, Bicyclic boronate VNRX-5133 inhibits metallo- and serine-β-lactamases, J. Med. Chem. 62 (2019) 8544–8556.

[18] B. Liu, R.E.L. Trout, G.-H. Chu, D. McGarry, R.W. Jackson, J.C. Hamrick, D.M. Daigle, S.M. Cusick, C. Pozzi, F. De Luca, M. Benvenuti, S. Mangani, J.-D. Docquier, W.J. Weiss, D.C. Pevear, L. Xerri, C.J. Burns, Discovery of taniborbactam (VNRX-5133): a broad-spectrum serine- and metallo-β-lactamase inhibitor for carbapenem-resistant bacterial infections, J. Med. Chem. 63 (2020) 2789–2801.

[19] Y. Xiang, Y.-J. Zhang, Y. Ge, Y. Zhou, C. Chen, W.Y. Wahlgren, X. Tan, X. Chen, K.-W. Yang, Kinetic, thermodynamic, and crystallographic studies of 2-triazolylthioacetamides as Verona integron-encoded metallo-β-lactamase 2 (VIM-2) inhibitor, Biomolecules 10 (2020) 72.

[20] C. Chen, K. Yang, Ruthenium complexes as prospective inhibitors of metallo-beta-lactamases to reverse carbapenem resistance, Dalton Trans. 49 (2020) 14099–14105.

[21] W.B. Jin, C. Xu, Q. Cheng, X.L. Qi, W. Gao, Z. Zheng, E.W.C. Chan, Y.-C. Leung, T.H. Chan, K.-Y. Wong, S. Chen, K.-F. Chan, Investigation of synergistic antimicrobial effects of the drug combinations of meropenem and 1,2-benzisoselenazol-3(2H)-one derivatives on carbapenem-resistant *enterobacteriaceae* producing NDM-1, Eur. J. Med. Chem. 155 (2018) 285–302.

[22] W.B. Jin, C. Xu, Q. Cheung, W. Gao, P. Zeng, J. Liu, E.W.C. Chan, Y.C. Leung, T.H. Chan, K.Y. Wong, S. Chen, K.F. Chan, Bioisosteric investigation of ebselen: synthesis and *in vitro* characterization of 1,2-benzisothiazol-3(2H)-one derivatives as potent New Delhi metallo-β-lactamase inhibitors, Bioorg. Chem. 100 (2020) 103873.

[23] G.-B. Li, M.I. Abboud, J. Brem, H. Someya, C.T. Lohans, S.-Y. Yang, J. Spencer, D.W. Wareham, M.A. McDonough, C.J. Schofield, NMR-filtered virtual screening leads to non-metal chelating metallo-β-lactamase inhibitors, Chem. Sci. 8 (2017) 928–937.

[24] Y. Wang, X. Sun, F. Kong, L. Xia, X. Deng, D. Wang, J. Wang, Specific NDM-1 inhibitor of isoliquiritin enhances the activity of meropenem against NDM-1-positive *Enterobacteriaceae in vitro*, Int. J. Environ. Res. Publ. Health 17 (2020) 2162.

[25] Y. Liu, K. Yang, Y. Jia, Z. Wang, Repurposing peptidomimetic as potential inhibitor of New Delhi metallo-beta-lactamases in gram-negative bacteria, ACS Infect. Dis. 5 (2019) 2061–2066.

[26] S. Liu, J. Zhang, Y. Zhou, N. Hu, J. Li, Y. Wang, X. Niu, X. Deng, J. Wang, Pterostilbene restores carbapenem susceptibility in New Delhi metallo-beta-lactamase-producing isolates by inhibiting the activity of New Delhi metallo-beta-lactamases, Br. J. Pharmacol. 176 (2019) 4548–4557.

[27] K. Tehrani, N.C. Bruchle, N. Wade, V. Mashayekhi, D. Pesce, M.J. van Haren, N.I. Martin, Small molecule carboxylates inhibit metallo-beta-lactamases and resensitize carbapenem-resistant bacteria to meropenem, ACS Infect. Dis. 6 (2020) 1366–1371.

[28] P.W. Kang, J.P. Su, L.Y. Sun, H. Gao, K.W. Yang, 3-Bromopyruvate as a potent covalently reversible inhibitor of New Delhi metallo-beta-lactamase-1 (NDM-1), Eur. J. Pharmaceut. Sci. 142 (2020) 105161.

[29] C. Schnaars, G. Kildahl-Andersen, A. Prandina, R. Popal, S. Radix, M. Le Borgne, T. Gjoen, A.M.S. Andresen, A. Heikal, O.A. Okstad, C. Frohlich, O. Samuelsen, S. Lauksund, L.P. Jordheim, P. Rongved, O.A.H. Astrand, Synthesis and preclinical evaluation of TPA-based zinc chelators as metallo-beta-lactamase inhibitors, ACS Infect. Dis. 4 (2018) 1407–1422.

[30] J.-i. Wachino, W. Jin, K. Kimura, H. Kurosaki, A. Sato, Y. Arakawa, Sulfamoyl heteroarylcarboxylic acids as promising metallo-β-lactamase inhibitors for controlling bacterial carbapenem resistance, mBio 11 (2020) e03144-03119.

[31] W. Chu, Y. Yang, J. Cai, H. Kong, M. Bai, X. Fu, S. Qin, E. Zhang, Synthesis and bioactivities of new membrane-active agents with aromatic linker: high selectivity and broad-spectrum antibacterial activity, ACS Infect. Dis. 5 (2019) 1535–1545.

[32] W. Chu, Y. Yang, S. Qin, J. Cai, M. Bai, H. Kong, E. Zhang, Low-toxicity amphiphilic molecules linked by an aromatic nucleus show broad-spectrum antibacterial activity and low drug resistance, Chem. Commun. 55 (2019) 4307–4310.

[33] M.M. Wang, W.C. Chu, Y. Yang, Q.Q. Yang, S.S. Qin, E. Zhang, Dithiocarbamates: efficient metallo-β-lactamase inhibitors with good antibacterial activity when combined with meropenem, Bioorg. Med. Chem. Lett 28 (2018) 3436–3440.

[34] E. Zhang, M.M. Wang, S.C. Huang, S.M. Xu, D.Y. Cui, Y.L. Bo, P.Y. Bai, Y.G. Hua, C.L. Xiao, S. Qin, NOTA analogue: a first dithiocarbamate inhibitor of metallo-beta-lactamases, Bioorg. Med. Chem. Lett 28 (2018) 214–221.

[35] X.F. Shi, M.M. Wang, S.C. Huang, J.X. Han, W.C. Chu, C. Xiao, E. Zhang, S. Qin, $H_2$depda: an acyclic adjuvant potentiates meropenem activity *in vitro* against metallo-beta-lactamase-producing *Enterobacterales*, Eur. J. Med. Chem. 167 (2019) 367–376.

[36] D.Y. Cui, Y. Yang, M.M. Bai, J.X. Han, C.C. Wang, H.T. Kong, B.Y. Shen, D.C. Yan, C.L. Xiao, Y.S. Liu, E. Zhang, Systematic research of $H_2$dedpa derivatives as potent inhibitors of New Delhi metallo-beta-lactamase-1, Bioorg. Chem. 101 (2020) 103965.

[37] D.M. Weekes, C.F. Ramogida, M.d.G. Jaraquemada-Peláez, B.O. Patrick, C. Apte, T.I. Kostelnik, J.F. Cawthray, L. Murphy, C. Orvig, Dipicolinate complexes of gallium(III) and lanthanum(III), Inorg. Chem. 55 (2016) 12544–12558.

[38] J. Brem, S.S. van Berkel, D. Zollman, S.Y. Lee, O. Gileadi, P.J. McHugh, T.R. Walsh, M.A. McDonough, C.J. Schofield, Structural basis of metallo-β-lactamase inhibition by captopril stereoisomers, Antimicrob. Agents Chemother. 60 (2016) 142–150.

[39] N. Aoki, Y. Ishii, K. Tateda, T. Saga, S. Kimura, Y. Kikuchi, T. Kobayashi, Y. Tanabe, H. Tsukada, F. Gejyo, K. Yamaguchi, Efficacy of calcium-EDTA as an inhibitor for metallo-β-lactamase in a mouse model of *Pseudomonas aeruginosa* pneumonia, Antimicrob. Agents Chemother. 54 (2010) 4582–4588.

[40] B. Kulengowski, D.S. Burgess, Imipenem/relebactam activity compared to other antimicrobials against non-MBL-producing carbapenem-resistant enterobacteriaceae from an academic medical center, Pathog Dis 77 (2019).

[41] J. Hoque, M.M. Konai, S. Gonuguntla, G.B. Manjunath, S. Samaddar, V. Yarlagadda, J. Haldar, Membrane active small molecules show selective broad spectrum antibacterial activity with No detectable resistance and eradicate biofilms, J. Med. Chem. 58 (2015) 5486–5500.

[42] K.B. Ishnava, P.P. Shah, Anticariogenic and hemolytic activity of selected seed protein extracts *In vitro* conditions, J. Dent. 11 (2014) 576–586.

[43] S. Qin, C. Zhang, S. Schwarz, L. Li, H. Dong, H. Yao, X.D. Du, Identification of a novel conjugative *mcr-8.2*-bearing plasmid in an almost pan-resistant hypermucoviscous *Klebsiella pneumoniae* ST11 isolate with enhanced virulence, J. Antimicrob. Chemother. 75 (2020) 2696–2699.

[44] T.W. Price, J. Gallo, V. Kubíček, Z. Böhmová, T.J. Prior, J. Greenman, P. Hermann, G.J. Stasiuk, Amino acid based gallium-68 chelators capable of radiolabeling at neutral pH, Dalton Trans. 46 (2017) 16973–16982.

[45] M. Khannam, S.K. Sahoo, C. Mukherjee, Effect of ligand chirality and hyperconjugation on the thermodynamic stability of a tris(aquated) GdIII complex: synthesis, characterization, and T1-weighted phantom MR image study, Eur. J. Inorg. Chem. (2019) 2518–2523, 2019.

[46] CLSI, Performance Standards for Antimicrobial Susceptibility Testing; 29th Informational Supplement. CLSI Document M100, CLSI, Wayne, PA, 2019.

[47] S.B. Falconer, S.A. Reid-Yu, A.M. King, S.S. Gehrke, W. Wang, J.F. Britten, B.K. Coombes, G.D. Wright, E.D. Brown, Zinc chelation by a small-molecule adjuvant potentiates meropenem activity *in vivo* against NDM-1-producing *Klebsiella pneumoniae*, ACS Infect. Dis. 1 (2015) 533–543.